

Automated drill-stop by SVM classified audible signals

Bernd M. Pohl^{1,2}, Jan O. Jungmann¹, Olaf Christ^{1,2} and Ulrich G. Hofmann³

Abstract—Neuroscience research often requires direct access to brain tissue in animal models which clearly requires opening of the protective cranium. Minimizing animal numbers requests only well-experienced surgeons, since clumsy performance may lead to premature death of the animal. To minimise those traumatic outcomes, an algorithmic approach for closed-loop control of our Spherical Assistant for Stereotaxic Surgery (SASSU) was designed. Controlling the surgical robot's micro-drill unit by audio pattern recognition proved to be a simple and reliable way to automatically stop the automated drill feed. Sound analysis based on the anatomical morphology of a rat skull was used to train a Support Vector Machine (SVM) classification of the time-frequency representations of the drill sound. Fully automated high throughput animal surgeries are the goal of this approach.

I. INTRODUCTION

Craniotomies in small animal surgeries are manually demanding procedures required for neurophysiological experiments to access brain matter. Common methods are rongeur [1] or manually drilling holes with miniature power drills into the animal's cranium [2], [3]. With these manipulations, it is very easy to induce stabbing wounds in the delicate tissue resulting in severe subcranial bleedings or death of the animal. Fig. 1 illustrates severe damage of a rat brain by a clumsy operator resulting in premature death of the animal. Recent developments in medical application bone drilling and breakthrough detection suggest to operate drilling via force or torque controlled drills [4], [5]. However, they require an expensive mechatronical set-up (price of force/torque sensors) and yield a time consuming procedure [2]. Additionally, in 2004, Boesnach et. al. developed a method for automated sound closed loop feedback controlled spine surgery and introduced special microphones into the operating theatre [6]. In order to minimise drill exposure, causing bone necrosis, tissue damage due to friction produced heat, and overcome time limitations [7], [8], a pattern recognition algorithm to control the drill by its sound production was designed in our study. The whole system will be part of a fully integrated Computer-Assisted-Surgery suite (CAS) [9] for small animals, based on our high precision spherical assistant for stereotactic surgeries (SASSU, promedTEC GmbH, Luebeck, Germany) [10].

*This work was supported by the Graduate School for Computing in Medicine and Life Sciences

¹Institute for Signal Processing, University of Luebeck, 23562 Luebeck, Germany www.isip.uni-luebeck.de

²Graduate School for Computing in Medicine and Life Sciences, University of Luebeck, Germany www.gradschool.uni-luebeck.de

³Research Group for Neuroelectronic Systems, Department of Neurosurgery, University Medical Center Freiburg, 79106 Freiburg, Germany ulrich.hofmann@coregen.uni-freiburg.de

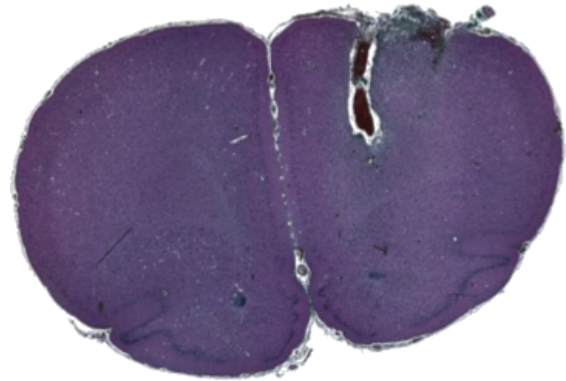


Fig. 1. Failed craniotomy: Power drill slipped in right hemisphere of the rat brain. Severe damage of brain caused premature death of animal.

II. MATERIALS AND METHODS

In this section, we describe the materials and methods applied in this study, subdivided into two parts: the preparation of small animal models and experimental setup, as well as the signal processing, pattern recognition and analysis involved. A number of ten experimental craniotomies in three rats were performed and audio files recorded.

A. Preparation of small animal model and experimental setup

Model animals used were approx. 280g heavy Wistar rat cadavers, left over from neurophysiological experiments, immediately after their planned euthanasia. Procedures performed implied a three point stereotactic fixation to the SASSU's built in frame, followed by surgical exposure of the skull along the sutura sagittalis. To access the periosteum and skull bone, each skin flap was tightened via medical sewing thread to the stereotaxic frame. To clean and visualise lambda and bregma for robotic navigation, the periosteum was scratched away and the skull surface area at lambda and bregma was bleached with 30% hydrogenperoxide. A dental drill station (NOUVAQ, Goldach, Switzerland) with a 0.8mm diameter spear point drill bit (Proxxon GmbH, Niersbach, Germany) was fixed to a custom made adapter for our stereotactic frame. Pre-positioning the drill bit to 2mm ventral, 2mm anterior of lambda close to the cranium, sound recording was started. SASSU's z-axis stepper motor moved the drill forward with a predefined velocity of 2mm/s, an acceleration of 3mm/s² and a z-axis displacement of 3mm. Audio data acquisition was performed via an external USB connected sound card (Edirol UA-25, Roland Corporation, Nakagawa, Japan), using a sampling frequency of 44.1kHz and maximum microphone gain sensitivity. Two electret

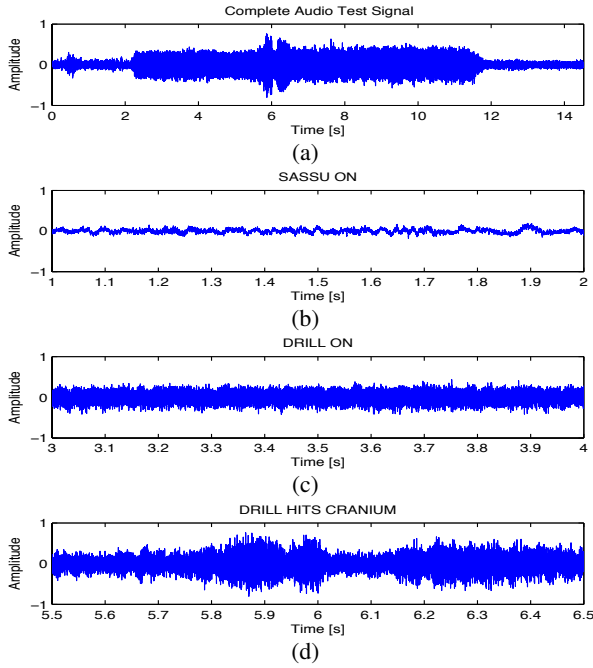


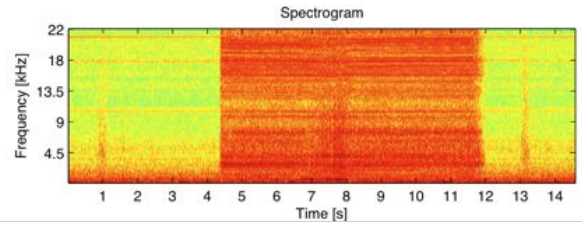
Fig. 2. Audio signal pattern classification: a) Complete audio signal, b) SASSU_ON class, c) DRILL_ON, d) DRILL_HITS_CRANIUM and breakthrough.

condenser measurement microphones with linear frequency response (MM1, Beyerdynamic, Heilbronn, Germany) were fixed to a microphone tripod 10cm away from the specimen. This close positioning minimised unwanted audio reverberation. Sound files were recorded with a freely available audio processing software (Audacity). For audio processing and data analysis, the Signal Processing Toolbox (The MathWorks Inc, Natick, Massachusetts, USA) was used. For SVM implementation the libSVM toolbox was used [11].

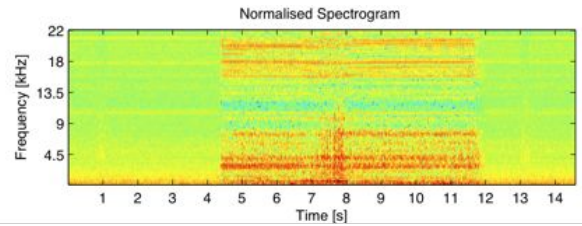
B. Signal Analysis

Experimental test data of ten craniotomies were converted into .wav files and each split into three classes, illustrated in Fig. 2. The raw audio signal is distinguishable into three classes, beginning with SASSU_ON. This stage captures SASSUs fan noise, followed by DRILL_ON and the actual performed craniotomy event - DRILL_HITS_CRANIUM. Each subfigure displays one second of each class. Out of ten sound files, spectrograms with weighted Hanning windows of 256 sample width, a shift of 128 samples and a Discrete Fourier Transformation (DFT) length of 256 samples, were generated. With this time-frequency representation, the spectral density of the signal can be estimated [12]. Displayed is a spectrogram of a sample audio drill procedure .wav file in Fig. 3 (a). We used the columns of the spectrogram as feature vectors. Each feature vector has a size of half the DFT length. For system robustness and comparability [13], [14], each feature vector was normalised so that its euclidean norm equaled to one (Fig. 3 (b)). A SVM classifier was trained on pre-recorded audio signals to calculate an offline model. The ability of SVMs to prevent overfitting and

simple separation of classes in feature space let us choose this method [14]. For the training data set of the SVM feature vector, borders were set manually. Out of the classes SASSU_ON and DRILL_ON, 500 vectors each, were used. Class three had maximum 50 feature vectors available due to preferable high speed drilling. For each training data matrix a same size vector containing the class labels was built. Depicted labels were allocated class 1,2 and 3, presenting the states of drilling procedure. Kernel function set to radial basis kernel (RBF). The RBF was selected, because of higher dimensional space mapping of our samples [14] resulting in high classification accuracy and its ability of handling a non-linear relation between class labels and attributes [15].



(a)



(b)

Fig. 3. Generated sample audio file spectrograms: (a) Audio File Spectrogram. (b) Normalised Spectrogram.

Using the labels, training data and parametric kernel options, the SVM model was calculated. Accuracy evaluation was done with none-trained data, ensuring that training- and test data set were disjoint. Accuracy measures were not calculated over the sum of all feature vectors, but each class was considered separately. To evaluate if our classifier is failing, the class-conditional error rates have to be analysed [16], with a confusion matrix [17] this is possible. It visualises the performance and recognition rate of the SVM classification of each separate class. In this, the actual and predicted classifications are shown. To minimise false classifications, the predicted labels were smoothed by voting. This additional post-processing step compared five predictions before and after the actual time index. Each classification was replaced by a voting with respect to its neighbours. This results in a suppression of outliers and therefore exploiting the temporal structure of the measured data, e.g. 111121111 = 1 or 1122222222 = 2 (Numbers represent classes).

III. RESULTS

An example of the drill recordings spectrogram is displayed in Fig. 4 (a). Three different time spans with characteristic frequency contents can be seen. During drilling,

DRILL_HITS_CRANIUM, two wide frequency bands with high energy are present. Feature vectors out of each audio file spectrogram were normalised with euclidean norm $\|x\|_2 = 1$ (Fig. 3 (b)) to make all audio recordings comparable [14]. Classification analysis was done with the help of a two modality method, a confusion matrix and the predicted label plot in comparison with unprocessed original raw audio data. The confusion matrix (Tab. I) shows the distribution of the feature vector classification. In total 1050 feature vectors were compared with their classification affiliation depending on the support vectors. A set of 500 disjoint test feature vectors, test data 1, was classified to 100% to class SASSU_ON. Followed by another 500 test feature vectors for class DRILL_ON, with an accuracy of another 100%. In class three, DRILL_HITS_CRANIUM, only 50 feature vectors were taken. This low restriction is due to the fact that the length of the time frames is a crucial problem in this pattern classification task. In this class, classification accuracy reached 92% before post-processing. Out of 50 feature vectors, 46 appendant to DRILL_HITS_CRANIUM and four were assigned to DRILL_ON. A comparison of predicted labels and spectrogram, based on the raw audio data can be seen in Fig. 4. The top plot (Fig. 4 (a)) illustrates the predicted labels of the test data over time in seconds. For comparison, all plots have the same x-axes scaling, time in seconds. False classified feature vectors were underlined with an oval black ellipse. Post-processed predicted labels, with classification voting, are displayed in Fig. 4 (c) leading to a visible reduction of false classified frames. Different states of the drilling procedure are emphasised with transparent blocks. The beginning and end white block illustrate an agreement of start and end time of the first class, SASSU_ON, followed by DRILL_ON and DRILL_HITS_CRANIUM. All plots show a strong correlation in time to the associated class and event.

TABLE I
TEST SIGNAL CLASSIFICATION RESULTS: CONFUSION MATRIX OF ACTUAL AND PREDICTED CLASSIFICATION. CLASS 1 AND CLASS 2 ACCURACY OF 100%. CLASS 3 46 FV ASSIGNED CORRECT AND 4 FALSE CLASSIFIED TO CLASS 2

	Test Data 1 [500FV]	Test Data 2 [500FV]	Test Data 3 [50FV]
SASSU_ON	500	0	0
DRILL_ON	0	500	4
DRILL_HITS_CRANIUM	0	0	46
Accuracy	100%	100%	92%

IV. DISCUSSION

The actual drilling procedure was performed with an 0.8mm diameter spear point drill. These drills are specifically designed for hard brittle materials, pearls, glass and ceramics. These machining abilities let us use it for bone drilling. The high z-axis velocity made sure that no slipping on the cranium surface occurred [2] and a smooth continuous

feed and bone chip removal [18] was assured. Previous experiments showed a slipping drill on the cranium, due to slow z-axis movement while using load cell evaluation [2]. In this cases oscillations occurred. In all audio files no oscillations were visible. Classes were selected by auditory and experimental methodology set-ups, initialising SASSU, switching on the power tool and bone drilling. All those actions resulted in a clear hearable distinguishable sound. At the event of DRILL_HITS_CRANIUM, the raw audio file showed an amplitude increase. However, rat skulls of different animals, like all biological structures, differ in size, thickness and morphology. Depending on the position of the drill on the cranium, either one enclosed or two separated hump/s were visible. We attribute this to the fact that the cranium, closer to the distal part of the skull, has a three layer anatomical structure consisting of the lamina externa, diploë and lamina interna. Drilled holes in the middle of the skull plate showed a to be neglected small diploë. Differences in amplitude or signal to noise ratio could not be recognised. Comparing the raw audio signal with the spectrogram (Fig. 4 (c) and Fig. 4 (d)) at times of events, a change in signal energy can be seen. Starting with the initialisation of SASSU, frequencies of 0 to 4.5kHz are predominant. This was associated to the SASSU's fan noise. At this time only the SASSU was on. Followed by the broad band noise of the power drill and the event of craniotomy. Normalising the feature vectors by the euclidean norm resulted in an equalisation of all audio recordings and made them comparable. This also enhanced the disparity in signal to noise ratio of DRILL_ON and DRILL_HITS_CRANIUM (Fig. 4). The confusion matrix showed a good classification of test data 1 and 2. However, class DRILL_HITS_CRANIUM was divergent and showed false classified frames. Out of 50 test feature vectors four were not associated with the correct class. We attribute this to the similarity in signal to noise ratio of the two classes and the few number of training feature vectors. We achieved a recognition rate of 92%. Fig. 4 showed additional validation of drill pattern recognition. At this step, a whole non-labeled audio file was classified. Clearly observable, was correct classification before and after the drill was switched on and off. At this state, the signal magnitude is highly differentiable between class DRILL_ON and DRILL_HITS_CRANIUM. The first white block illustrates the co-occurrence of class 1 (SASSU_ON) and the raw audio data state at the same time. First grey block show class 2, DRILL_ON. A slight change in signal amplitude is visible and was attributed to vibrations due to drill bit rotation in the sub-cranial cavity. At this state, false classified frames occur due to not clearly distinguishable frequency distributions. However these false classified frames occurred only occasionally and hardly represent a false classification. During the drilling period the predicted class 3, DRILL_HITS_CRANIUM is subdivided into two classes. Class 3 is predicted as long as the drill penetrates the lamina externa. In the subsequent process, class 2 is dominant and again the classification changes to class 3. We assign this peculiar sound behaviour to the three layer anatomical rat skull structure. At the end of the second

grey block, 11.5s in Fig. 4 (c) and (d), a smoothing out of the signal can be seen. At this time the drill was switched of and a machine run-out occurred. Post-processing of classification by voting resulted in Fig. 4 (b). False classified frames were associated to its predominant class and reduced the amount of false classified feature vectors. Overall, the distinguishing patterns were trackable in all recorded .wav files and showed a strong connection with the three layer anatomical structure of the rat cranium [2]. This time frequency analysis gave a good perspective to overcome classification errors and is the method for further investigations. In this study we showed a classification procedure for automatised, closed loop craniotomies in small animal neuro-surgeries. Comparing the load cell results, discussed in [2], with the audio analysis breakthrough detection, showed a strong correlation of the morphology of the rat cranium. The audio analysis promises better outcomes and a higher performance. High z-axis drill feed reduced methodology time to produce one hole from 7.5min, load cell drilling, to under a second with audio controlled closed loop. Furthermore, it must be stated, that the additional signal processing is needed for a real application. In case of stray sounds, detailed frequency analysis is an unavoidable necessity to prevent false classification.

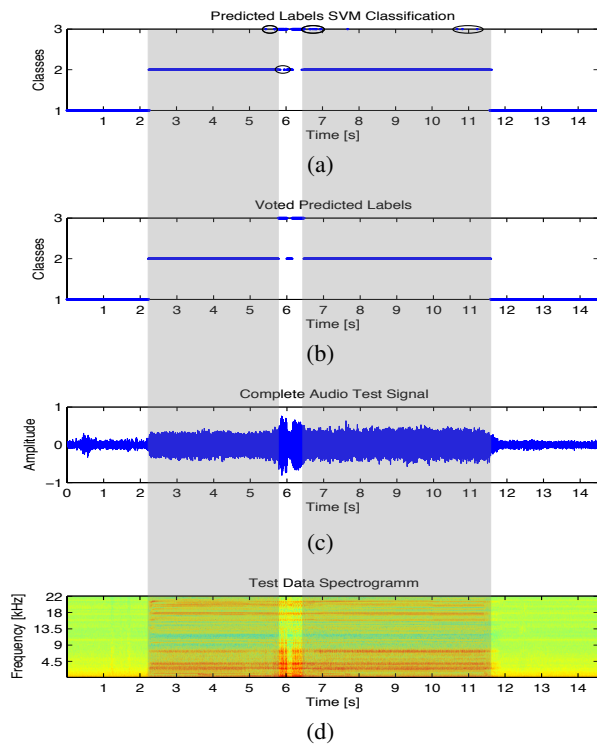


Fig. 4. Comparison of pattern recognition: (a) Predicted labels SVM classification, (b) Voted predicted labels, (c) Complete audio test signal, (d) Test data spectrogram

V. OUTLOOK

In this study we showed a strong link between the original recorded audio files and several events while drilling through

rat skull bone. This approach will be used to run an automated drilling procedure in our integrated robotic assisted surgery suite. Adaptive filtering and data cross validation is under investigation to improve system robustness and biological variation adaptation. This will open the path to closed loop minimal trauma craniotomies.

ACKNOWLEDGEMENT

This work was supported by the Graduate School for Computing in Medicine and Life Sciences funded by Germanys Excellence Initiative [DFG, GSC 235/1]. Many thanks is dedicated to Florian Müller, Institute for Signal Processing, for hours of discussion and theoretical background knowledge.

REFERENCES

- [1] F. M. Swaim. A rongeur technique for performing thoracolumbar hemilaminectomies. *Vet Med Small Anim Clin.*, 71(2):172–5, 1976.
- [2] B. M. Pohl, A. Schumacher, and U. G. Hofmann. Towards an automated, minimal invasive, precision craniotomy on small animals. In *5th International IEEE/EMBS Conference on Neural Engineering (NER)*, 2011.
- [3] M. Schwindle H. Elliot H.B. Waynforth and A. Smith. *Handbook of Laboratory Animal Science Essential Principles and Practices*. CRC Press LLC, 2003.
- [4] C. J. Coulson. An autonomous surgical robot for drilling an cochleostomy: preliminary porcine trial. *Clinical Otolaryngology*, Volume 33, Issue 4:pages 343–347, 2008.
- [5] Hao-Wei Yeh-Liang, Shih-Tseng. A modular mechatronic system for automatic bone drilling. *Biomedical Engineering Application Basis and Communications*, 13:168–174, 2001.
- [6] I. Boesnach, M. Hahn, J. Moldenhauer, and Th. Beth. Analysis of drill sound in spine surgery. In *Perspective in Image guided Surgery*, 2004.
- [7] I. Shuaib M. T. Hillery. Temperature effects in the drilling of human and bovine bone. *Journal of Materials Processing Technology*, pages 92–93, 1999.
- [8] S. Skoric T. Udiljak, D. Ciglar. Investigation into bone drilling and thermal bone necrosis. *Advances in production Engineering and Management*, Vol. 3:103–112, 2007.
- [9] Ching-Long Shih Wen-Yo Lee. Force control breakthrough detection of bone drilling system. In *Internation Conference on Robotics and Automation*, 2003.
- [10] L. Ramrath, U.G. Hofmann, and A. Schweikard. A robotic assistant for seroetactic neurosurgery on small animals. *Int. Journal on Medical Robotics and Computer Assisted Surgery*, 4(4):295–303, 2008.
- [11] C. Chang and C. Lin. Libsvm: a library for support vector machines. *ACM Transactions on Intelligent Systems and Technology*, pages 1–27, 2011.
- [12] S. Haykin. *Advances in Spectrum Analysis and Array Processing*, volume Vol.1. Prentice-Hall, 1991.
- [13] D. S. Sivia, editor. *Data Analysis - A Bayesian Tutorial*. Oxford University Press, 1997.
- [14] S. Abe. *Pattern Classification: Neuro-fuzzy Methods and Their Comparison*. Springer-Verlag London Limited, 2001.
- [15] Chih-Wei Hsu, Chih-Chung Chang, and Chih-Jen Lin. A practical guide to support vector classification. Technical report, Department of Computer Science, National Taiwan University, Taipei 106, Taiwan, April 2010.
- [16] B. D. Ripley. *Pattern Recognition and Neural Networks*. Cambridge University Press, 1996.
- [17] R. Kohavi and F. Provost. Glossary of terms:editorial for the special issue on applications of machine learning and the knowledge discovery process. *Machine Learning*, 30:(2–3), 1998.
- [18] M. P. Groover. *Fundamentals of Modern Manufacturing: Materials, Processes and Systems*. John Wiley & Sons, 2007.